

## **Imaging System Performance and Visibility as Affected by the Physical Environment**

Grace Chang  
Sea Engineering, Inc.  
200 Washington St., Suite 210  
Santa Cruz, CA 95060  
Phone: (831) 421-0871   Fax: (831) 421-0875   Email: [gchang@seaengineering.com](mailto:gchang@seaengineering.com)

Award Number: N00014-11-M-0144

### **LONG-TERM GOALS**

The long-term goal of “Imaging System Performance and Visibility as Affected by the Physical Environment” is to investigate the relationships between physical forcing and optical properties, including the imaging performance parameters. Our efforts are aimed at supporting the Radiance in a Dynamic Ocean (RaDyO) program, which is devoted to the topic of light propagation and imaging across the air-sea interface and within the surface boundary layer of natural water bodies.

### **OBJECTIVES**

The objectives of this project are to:

- Determine the relationships between physical processes and the optical properties that affect underwater visibility and the imaging performance parameters (Chang and Twardowski, 2011).
- Investigate the effects of vertical variability (e.g., vertical layering) of optical properties on the image performance parameter, the modulation transfer function (MTF).

Here, we discuss the MTF of a relatively clear, deep water, mesotrophic environment and address the following issues:

- How scattering layers and their relative positions from detectors and targets affect the MTF.
- To what degree image reconstruction is compromised by MTFs computed for optically homogeneous versus optically inhomogeneous waters.

### **APPROACH**

The MTF of seawater was computed using profiled measurements of inherent optical properties (IOPs) conducted between the near-surface and 30 m water depth in the Santa Barbara Channel (SBC) as part of the ONR RaDyO project (see Chang et al., 2010 and Chang and Twardowski, 2011). The data IOP processing approach utilized factory-recommended and published calibration and correction procedures for IOP sensors (e.g., Zaneveld et al., 1994; Pegau et al., 1997; Sullivan et al., 2006; Zhang

<b>Report Documentation Page</b>			Form Approved OMB No. 0704-0188	
<p>Public reporting burden for the collection of information is estimated to average 1 hour per response, including the time for reviewing instructions, searching existing data sources, gathering and maintaining the data needed, and completing and reviewing the collection of information. Send comments regarding this burden estimate or any other aspect of this collection of information, including suggestions for reducing this burden, to Washington Headquarters Services, Directorate for Information Operations and Reports, 1215 Jefferson Davis Highway, Suite 1204, Arlington VA 22202-4302. Respondents should be aware that notwithstanding any other provision of law, no person shall be subject to a penalty for failing to comply with a collection of information if it does not display a currently valid OMB control number.</p>				
1. REPORT DATE <b>2012</b>	2. REPORT TYPE <b>N/A</b>	3. DATES COVERED <b>-</b>		
<b>4. TITLE AND SUBTITLE</b> <b>Imaging System Performance and Visibility as Affected by the Physical Environment</b>			5a. CONTRACT NUMBER	
			5b. GRANT NUMBER	
			5c. PROGRAM ELEMENT NUMBER	
<b>6. AUTHOR(S)</b>			5d. PROJECT NUMBER	
			5e. TASK NUMBER	
			5f. WORK UNIT NUMBER	
<b>7. PERFORMING ORGANIZATION NAME(S) AND ADDRESS(ES)</b> <b>Sea Engineering, Inc. 200 Washington St., Suite 210 Santa Cruz, CA 95060</b>			8. PERFORMING ORGANIZATION REPORT NUMBER	
<b>9. SPONSORING/MONITORING AGENCY NAME(S) AND ADDRESS(ES)</b>			10. SPONSOR/MONITOR'S ACRONYM(S)	
			11. SPONSOR/MONITOR'S REPORT NUMBER(S)	
<b>12. DISTRIBUTION/AVAILABILITY STATEMENT</b> <b>Approved for public release, distribution unlimited</b>				
<b>13. SUPPLEMENTARY NOTES</b> <b>The original document contains color images.</b>				
<b>14. ABSTRACT</b>				
<b>15. SUBJECT TERMS</b>				
<b>16. SECURITY CLASSIFICATION OF:</b>			<b>17. LIMITATION OF ABSTRACT</b> <b>SAR</b>	<b>18. NUMBER OF PAGES</b> <b>6</b>
a. REPORT <b>unclassified</b>	b. ABSTRACT <b>unclassified</b>	c. THIS PAGE <b>unclassified</b>		

et al., 2009). The effects of stratification and scattering layers on the MTF were examined for two different scenarios (Figure 1):

- A virtual imager located at the surface and virtual targets at ranges between 10 cm and 30 m below the source.
- Virtual imagers located between the surface and 30 m and the targets located 10 cm below the imagers.

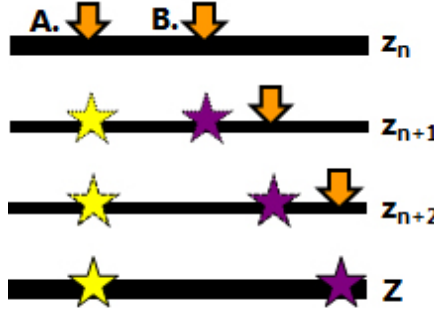


**Figure 1. Schematic diagram of two scenarios: A (left). Virtual imager (arrow) and virtual targets (stars) separated by scattering layers,  $z_n$ , over a total distance,  $Z$ , and B (right). Virtual imagers located a distance,  $z_n$ , above virtual targets.**

## WORK COMPLETED

For scenario A (Figure 1, left), the collimated decay transfer function (DTF),  $D^c(\Psi)$ , and MTF,  $H(\Psi)$ , at range,  $Z$ , and spatial frequency,  $\psi$ , were computed following:

$$D^c(\Psi)_s = c - \int_{z_1/Z}^{z_2/Z} S(\Psi, z) dz$$

where the  $s$  denotes the scattering layer,  $c$  is the beam attenuation coefficient of layer  $s$ ,  $S$  is the light scattered back to the acceptance cone of layer  $s$ , and an integral taken between the imager and distances  $z_1$  and  $z_2$  over a total range of  $Z$  to the target.

$$S(\Psi) = 2\pi \int_0^{\theta_{\max}} J_0(2\pi\theta\Psi) \beta(\theta) \theta d\theta$$

where  $\beta(\theta)$  is the volume scattering function (VSF),  $\theta$  is the scattering angle, and  $J_0$  is the zero-order Bessel function. The near-forward VSF was measured using a LISST-100X and measurements of the beam attenuation coefficient were provided by an ac-s. The focused DTF was obtained by transformation in terms of spatial frequency ( $2\pi\theta\Psi$ ) prior to computation of the MTF (Wells, 1973):

$$D(\Psi) = \int_0^1 D^c(\Psi t) dt$$

$$H(\Psi, z)_s = e^{-[D_1(\Psi)Z_1 + D_2(\Psi)Z_2 + \dots]}$$

Vertical profiles of the MTF at a spatial frequency equal to  $1.0 \text{ rad}^{-1}$  were constructed using the equation for  $H(\Psi, z)_s$  above by summing the DTFs between the surface and each  $z_n = 10 \text{ cm}$  layer to a maximum range of  $Z = 30 \text{ m}$  (Figure 2).

The DTF and MTF for scenario B (Figure 1, right) were calculated following:

$$D(\psi) = c - S(\psi)$$

$$H(\psi, z) = e^{-D(\psi)z}$$

where  $z$  is the range of each layer (e.g.,  $z_{n+2}$  to  $Z$ ), with similar transformation to the focused DTF. In case B, the vertical profile of the MTF for  $\psi$  equal to  $1.0 \text{ rad}^{-1}$  was constructed with multiple virtual imagers and targets, all separated by the same distance (10 cm) (Figure 1).

Scattering layer effects on the MTF for the two different scenarios were quantified by:

- 1) Applying a power-law fit,  $\gamma$ , to the MTF at a given spatial frequency as a function of depth.
- 2) Determining the extinction depth,  $\kappa$ , of MTF, where the extinction depth was defined as the depth at which the MTF decreased to 0.01 cycles/rad.

## RESULTS

The upper water column MTF at small spatial frequencies in the presence of scattering layers and stratification can be orders of magnitude less than the MTF in mixed conditions, as illustrated in Figure 2. The distance between the imager and target contributed greatly to the magnitude of the MTF when imager and target were separated by a scattering layer.

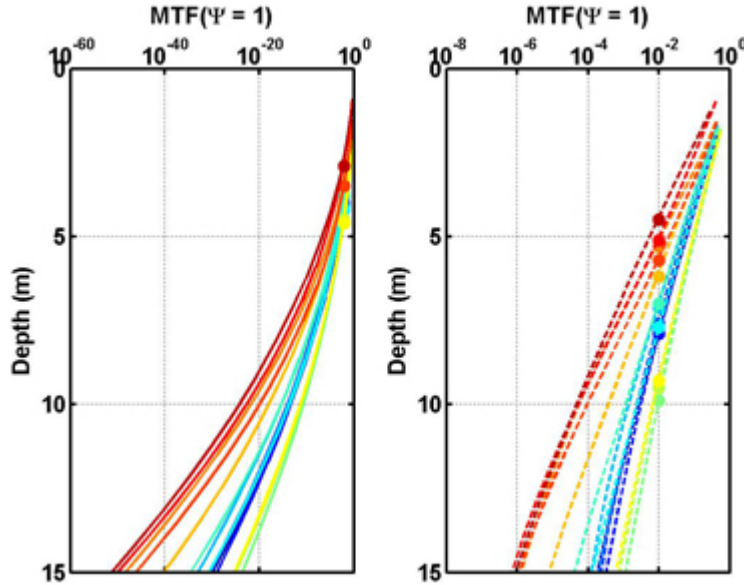


*Figure 2. Vertical profiles of the MTF( $\Psi = 1 \text{ rad}^{-1}$ ) shown to a range of  $Z = 15 \text{ m}$  for A: Scenario A and B: Scenario B. The solid dots indicate the extinction depth,  $\kappa$ . Profile color-coding denotes specific periods of the SBC RaDyO experiment: blues = strong stratification, yellow-green = upper water column mixing, and reds = strong scattering layers from localized upwelling (see Chang et al., 2010 and Chang and Twardowski, 2011 for more details).*

The extinction depth determined for the MTF( $\Psi = 1 \text{ rad}^{-1}$ ) with an imager at the surface (scenario A) did not vary greatly from about 4.5 m for all 15 profiles; the minimum value of  $\kappa$  was 2.9 m in the presence of strong scattering layers and maximum  $\kappa$  was 4.8 m during mixed conditions (Figure 3). When virtual imagers and targets were placed 10 cm apart throughout the water column,  $\kappa$  varied between 4.5 m (strong scattering layers) and 9.8 m (mixed conditions).

The differences in  $\gamma$  between scenarios A and B were larger during stratified conditions (average difference of 1.5) as compared to during upper water column mixed conditions (average difference of 1.25). The smallest difference in  $\gamma$  between scenarios A and B (0.985) occurred during periods with strong scattering layers (Figure 3).

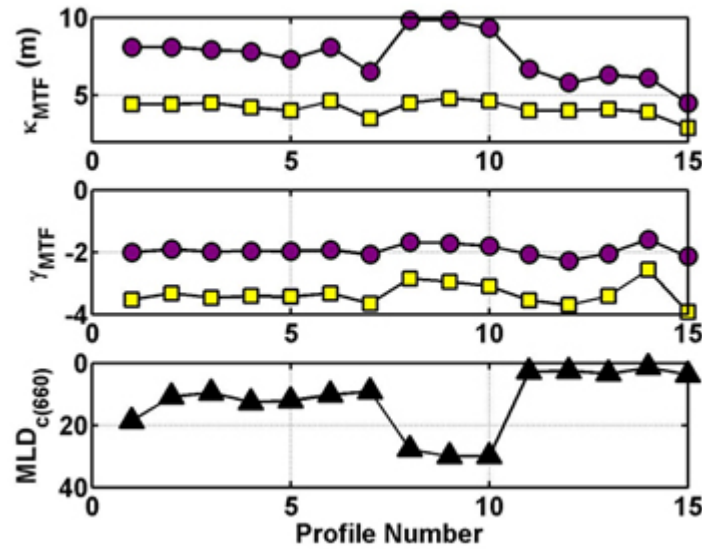


**Figure 3.** Upper: MTF( $\Psi = 1 \text{ rad}^{-1}$ ) extinction depth, Middle: Slope of the power-law fit to the vertical profile of MTF( $\Psi = 1 \text{ rad}^{-1}$ ), and Lower: The mixed layer depth computed as the depth at which the  $c_{\text{pg}}(660)$  change from near-surface  $c_{\text{pg}}(660)$  is greater than  $0.05 \text{ m}^{-1}$ . Yellow = scenario A and Purple = scenario B. The profile numbers can be characterized by: 1-7 = strong stratification, 8-10 = mixed, and 11-15 = strong scattering layers.

These results imply that in the presence of near-surface optical scattering layers, an underwater image taken from just below the surface to a depth of a mere 0.5 m can be significantly blurrier than if the imager was located tens of cm below the surface. Additionally, analysis or reconstruction of an image taken by a near-surface detector of a target located at just a couple of meters below the surface may not be possible in the presence of strong scattering layers, even if the water appears relatively clear from the surface.

## IMPACT/APPLICATIONS

Knowledge of the MTF is important for the interpretation of images from underwater electro-optical imaging systems. MTF-based image analysis and reconstruction is influenced by optical inhomogeneity (i.e. scattering layers) as well as by the vertical placement of the target versus that of the detector, or imager (Wells, 1973; Frew and Voss, 1997). Take, for example, the remark made by

Wells (1973), “You can lay a sheet of vellum on a printed page and read through it quite well, but the same vellum lifted a centimeter off the page completely obscures vision.” This statement is now outdated as vellum is no longer a common source for paper. Here is another way to consider the problem: one should not feel embarrassed while showering several feet away from a textured shower door; however body parts could be fully revealed should they make contact with the door (Figure 4).

This same effect applies in stratified ocean environments where a target and imager are separated by optically distinct layers. These layers could have important implications on imaging performance and analysis. The ability to determine optimal placement of passive imagers relative to target locations would constitute dramatic improvements to image clarity and restoration efforts. Additionally, image reconstruction would be facilitated with knowledge of the effects of scattering layers on image distortion and imaging performance parameters.

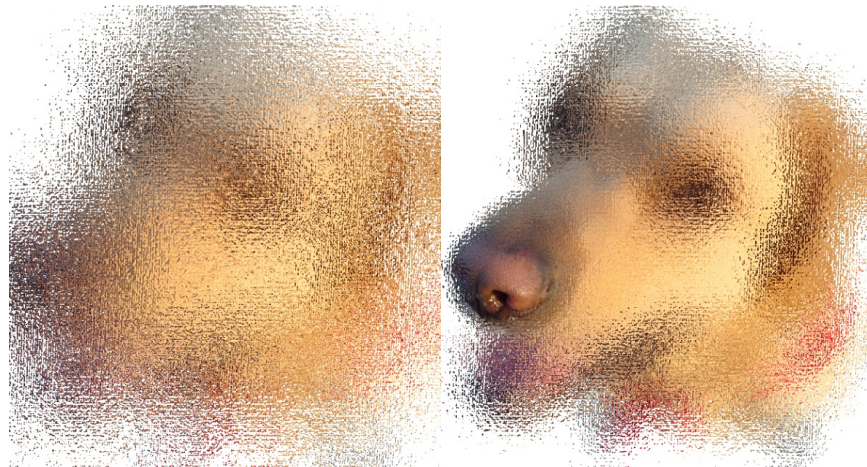


**Figure 4.** These photographs of Peso the dog were manipulated in Photoshop to simulate Peso well behind a textured glass shower door (Left) and Peso’s nose pressed against the glass (Right).

## RELATED PROJECTS

None

## REFERENCES

- Chang, G. and M. S. Twardowski (2011) Effects of physical forcing and particle characteristics on underwater imaging performance, *J. Geophys. Res.*, 116, C00H03, doi:10.1029/2011JC007098.
- Chang, G., M. S. Twardowski, Y. You, M. Moline, P.-W. Zhai, S. Freeman, M. Slivkoff, F. Nencioli, and G. W. Kattawar (2010) Platform effects on optical variability and prediction of underwater visibility, *Appl. Opt.*, 49(15), 2784-2796.
- Frew, B. and K. Voss (1997) Measurement of the point-spread function in a layered system, *Appl. Opt.*, 36, 3335-3337.
- Pegau, W. S., D. Gray, and J. R. V. Zaneveld (1997) Absorption and attenuation of visible and near-infrared light in water: dependence on temperature and salinity, *Appl. Opt.*, 36, 6035-6046.

- Sullivan, J. M., M. S. Twardowski, J. R. V. Zaneveld, C. M. Moore, A. H. Barnard, P. L. Donaghay, and B. Rhoades (2006) Hyperspectral temperature and salt dependencies of absorption by water and heavy water in the 400-750 nm spectral range, *Appl. Opt.*, 45, 5294-5309.
- Wells, W. H. (1973) Theory of small angle scattering, in AGARD Lec. Series No. 61, pp. 3.3.1 – 3.3.19, NATO, Neuilly-sur-Seine, France.
- Zaneveld, J. R. V., J. C. Kitchen, and C. M. Moore (1994) Scattering error correction of reflecting-tube absorption meters, in *Ocean Optics XII*, J. S. Jeffe (Ed.), Proc. SPIE 2258, 44-55.
- Zhang, X., L. Hu, and M-X. He (2009) Scattering by pure seawater: Effect of salinity, *Opt. Expr.*, 17, 5698-5710.

## PUBLICATIONS

- Chang, G., M. S. Twardowski, Y. You, M. Moline, P.-W. Zhai, S. Freeman, M. Slivkoff, F. Nencioli, and G. W. Kattawar (2010) Platform effects on optical variability and prediction of underwater visibility, *Appl. Opt.*, 49(15), 2784-2796. [Published, Refereed]
- Chang, G. and M. S. Twardowski (2011) Effects of physical forcing and particle characteristics on underwater imaging performance, *J. Geophys. Res.*, 116, C00H03, doi:10.1029/2011JC007098. [Published, Refereed]
- Chang, G. (2012) Scattering layer effects on the modulation transfer function, Proceedings of the Ocean Optics Conference (extended abstract), Glasgow, Scotland, October 2012.